

Near-threshold production of ω mesons in the $pn \rightarrow d\omega$ reaction

S. Barsov¹, I. Lehmann², R. Schleichert^{2a}, C. Wilkin³, M. Büscher², S. Dymov^{2,4}, Ye. Golubeva⁵, M. Hartmann², V. Hejny², A. Kacharava⁶, I. Keshelashvili^{2,6}, A. Khoukaz⁷, V. Komarov⁴, L. Kondratyuk⁸, N. Lang⁷, G. Macharashvili^{4,6}, T. Mersmann⁷, S. Merzlikov⁴, A. Mussgiller², M. Nioradze⁶, A. Petrus⁴, H. Ströher², Y. Uzikov⁴, and B. Zalikhanov⁴

¹ High Energy Physics Department, Petersburg Nuclear Physics Institute, 188350 Gatchina, Russia

² Institut für Kernphysik, Forschungszentrum Jülich, D-52425 Jülich, Germany

³ Physics & Astronomy Department, UCL, Gower Street, London WC1E 6BT, UK

⁴ Laboratory of Nuclear Problems, Joint Institute for Nuclear Research, Dubna, 141980 Dubna, Russia

⁵ Institute for Nuclear Research, Russian Academy of Sciences, 117312 Moscow, Russia

⁶ High Energy Physics Institute, Tbilisi State University, University Street 9, 380086 Tbilisi, Georgia

⁷ Institut für Kernphysik, Universität Münster, W.-Klemm-Street 9, 48149 Münster, Germany

⁸ Institute for Theoretical and Experimental Physics, Chermushkinskaya 25, 117259 Moscow, Russia

Received: November 8, 2018/ Revised version: date

Abstract. The first measurement of the $pn \rightarrow d\omega$ total cross section has been achieved at mean excess energies of $Q \approx 28$ and 57 MeV by using a deuterium cluster-jet target. The momentum of the fast deuteron was measured in the ANKE spectrometer at COSY-Jülich and that of the slow “spectator” proton (p_{sp}) from the $pd \rightarrow p_{\text{sp}}d\omega$ reaction in a silicon telescope placed close to the target. The cross sections lie above those measured for $pp \rightarrow pp\omega$ but seem to be below theoretical predictions.

PACS. 25.40.Ve Other reactions above meson production thresholds (Energies > 400 MeV) – 25.40.Fq Inelastic neutron scattering – 14.40.Cs Other mesons with $S = C = 0$, mass < 2.5 GeV

1 Introduction

The last few years have seen several measurements of η production in nucleon-nucleon collisions [1] but relatively few of ω production [2, 3]. The S -wave amplitude in the η case is strong and the total $pp \rightarrow pp\eta$ cross section largely follows phase space modified by the pp final state interaction up to an excess energy $Q = \sqrt{s} - \sum_f m_f \approx 60$ MeV, though there is some evidence for an ηpp final state enhancement at very low Q [4]. Here \sqrt{s} is the total centre-of-mass (cm) energy and m_f are the masses of the particles in the final state. Quasi-free η production in proton-neutron collisions has been measured by detecting the photons from η decay and it is found that for $Q < 100$ MeV the cross section ratio $R = \sigma_{\text{tot}}(pn \rightarrow pn\eta)/\sigma_{\text{tot}}(pp \rightarrow pp\eta) \approx 6.5$ [5]. Now the $d\eta$ final state is pure isospin $I = 0$, whereas the $pp\eta$ is a mixture of $I = 0$ and $I = 1$. Up to $Q \approx 60$ MeV the cross section for $pn \rightarrow d\eta$ is larger than that for $pn \rightarrow pn\eta$ [6], and this can be understood quantitatively in terms of phase space in a largely model-independent way [4]. In all meson production reactions it is important to have data on the different possible isospin combinations in order to constrain theoretical models. It is therefore interesting to see whether a similar isospin

dependence is found for the ω , the next heavier isoscalar meson.

Unlike the η case, the ω -meson has a significant width (8.4 MeV/ c^2) and so Q is here defined with respect to the central mass value of 782.6 MeV/ c^2 [7]. The $pp \rightarrow pp\omega$ total cross section has been measured at five energies in the range $4 \leq Q \leq 30$ MeV at the SATURNE SPESIII spectrometer [2] and at $Q = 92$ MeV at COSY-TOF [3] where, in both cases, the ω was identified through the missing mass technique. The energy dependence deduced is rather similar to that of the η , except that the phase space and pp final state interaction have to be smeared over the finite ω width, a feature which becomes important close to the nominal threshold [2].

Attempts to measure the $np \rightarrow d\omega$ reaction using a neutron beam are complicated by the intrinsic momentum spread, which is typically 7% FWHM even for a stripped deuteron beam [8]. The alternative is to use a deuterium target and effectively measure the momentum of the struck neutron. This is made possible by detecting the very low momentum recoil protons, $\lesssim 200$ MeV/ c , in the $pd \rightarrow p_{\text{sp}}d\omega$ reaction in a silicon telescope placed close to the target. Such an approach is feasible at internal experiments at storage rings such as CELSIUS or COSY because of the thin windowless targets that can be used there. Under these conditions the recoil proton can be

^a E-mail: r.schleichert@fz-juelich.de

largely treated as a “spectator” that only enters the reaction through its modification of the kinematics. The measurement of the fast deuteron in coincidence would then allow us to identify the ω by the missing mass method. By varying the angle and momentum of the spectator proton it is possible to change the value of Q while keeping the beam momentum fixed. The principle of this method has been proved at CELSIUS for the $pn \rightarrow d\pi^0$ reaction, where Q could be determined to 2 MeV [9].

2 Experimental Set-up

Our experiment was performed using a deuterium cluster-jet target [10] at the ANKE spectrometer [11] situated inside the COoler SYnchrotron COSY-Jülich, with the fast deuteron being measured in the ANKE Forward Detector and the spectator proton in solid state counters. The silicon telescope used for this purpose is described in detail in Ref. [12] and only the principal features will be mentioned here. The three silicon layers indicated in Fig. 1, of respectively $60\ \mu\text{m}$, $300\ \mu\text{m}$, and $5\ \text{mm}$, covered polar angles $83^\circ < \theta_{\text{sp}} < 104^\circ$ and $\pm 7^\circ$ in azimuth. Protons with kinetic energies T_{sp} in the range 2 – 6 MeV traversed the first layer but were stopped in the second, while those in the range 6 – 30 MeV were stopped rather in the final thick layer. Energy resolution of the order of $\sigma = 150\ \text{keV}$ was obtained. The second and third layers were composed of strips arranged perpendicular to the beam such that for $T_{\text{sp}} > 8\ \text{MeV}$ a resolution of $\sigma(\theta_{\text{sp}}) \leq 3^\circ$ could be achieved. For the lower energy protons, neglecting the small non-target background, the finite target size led to $\sigma(\theta_{\text{sp}}) \leq 5^\circ$.

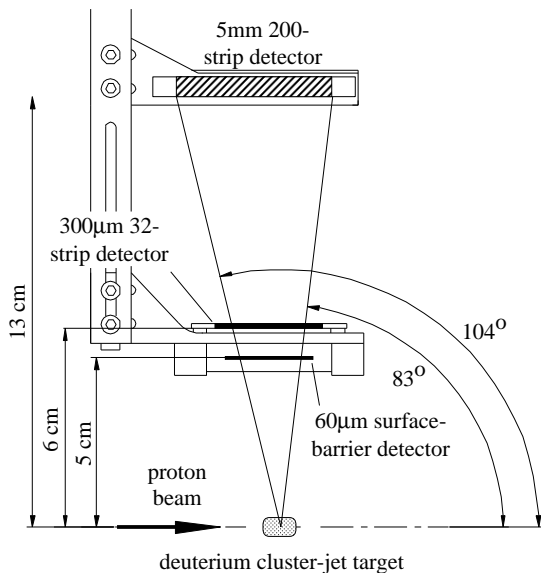


Fig. 1. Top view of the telescope placed close to the deuterium cluster-jet target inside the vacuum chamber of ANKE. Protons and deuterons emerging from the beam-target overlap region (shaded area) are detected in the subsequent arrangement of three silicon detectors (see text).

There was no difficulty in separating slow deuterons from protons *via* the $E - \Delta E$ method in two ranges: $2.6 < T_{\text{sp}} < 4.4\ \text{MeV}$ ($70 < p_{\text{sp}} < 91\ \text{MeV}/c$) and also $8 < T_{\text{sp}} < 22\ \text{MeV}$ ($123 < p_{\text{sp}} < 204\ \text{MeV}/c$). This is illustrated for the lower range in Fig. 2. It is seen here that, by choosing the 4.4 MeV upper limit, one avoids the possibility of misidentifying deuterons traversing the first two layers but missing the third.

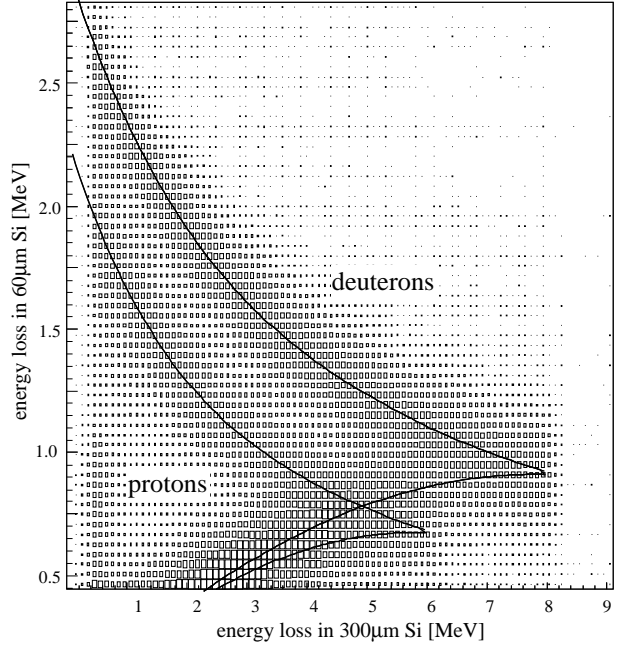


Fig. 2. Particle identification *via* their energy deposit in the first two detectors of the telescope. Boxes corresponding to experimental data are compared to curves predicted for protons and deuterons.

The ability to identify a deuteron in the telescope in coincidence with a proton in the forward detector also allows us to obtain simultaneously the luminosity by measuring proton-deuteron elastic scattering through a determination of the deuteron kinetic energy. For this purpose we have calculated the elastic proton-deuteron cross section at our energies within the Glauber model [13]. Such an estimate agrees with the available experimental $pd \rightarrow pd$ data at 2.78 GeV/c to within the quoted error of about 10% [14]. The 1% uncertainty in the energy of the recoil deuteron, and hence in the momentum transfer, induces only a 3% error through the angular variation of the normalising reaction. Due to uncertainties in the geometrical constraints in the target chamber, the acceptance correction introduces a 15% systematic error in the absolute cross section normalisation. The overall systematic luminosity error used to determine absolute cross sections was thus taken to be 20%. It should be noted, however, that the error in the relative normalisation between different beam energies is at most 5%.

In order to distinguish deuterons with momenta around 2 GeV/c, arising from the $pd \rightarrow p_{\text{sp}}d\omega$ reaction, from a

proton background that is two orders of magnitude higher, inclined Čerenkov counters were installed behind the multi-wire proportional chambers and scintillator hodoscope of the forward detection system of ANKE [11,15]. To understand the detection principle, consider the detector response for a proton and deuteron with the same momentum. The opening angle of the Čerenkov light cone for the faster proton is larger. Thus part of the light can reach the photomultiplier after being totally reflected in the counter, whereas all the light produced by the deuteron leaves the counter. A momentum-dependent threshold was applied so as not to change the differential distributions.

The hodoscope, consisting of two layers of scintillation counters, provides an additional criterion for the deuteron identification using the energy loss in both layers. By simultaneously varying the ΔE -cut and Čerenkov efficiency level, an optimal combination was found which leads to only a 20% loss of deuterons while giving a 92% suppression of protons due to the Čerenkov counters alone. Projecting the energy loss in the second layer along the predicted energy loss of deuterons ($\propto \beta_d^{-2}$), one obtains the dotted histogram shown in Fig. 3. A further cut on the analogous distribution in the first layer reveals a clear deuteron peak (solid line). Moreover, the shape of the remaining proton background can be determined using the energy loss distribution of suppressed particles which, after scaling, is drawn as the dashed line. This shows that the proton background is on the 10% level.

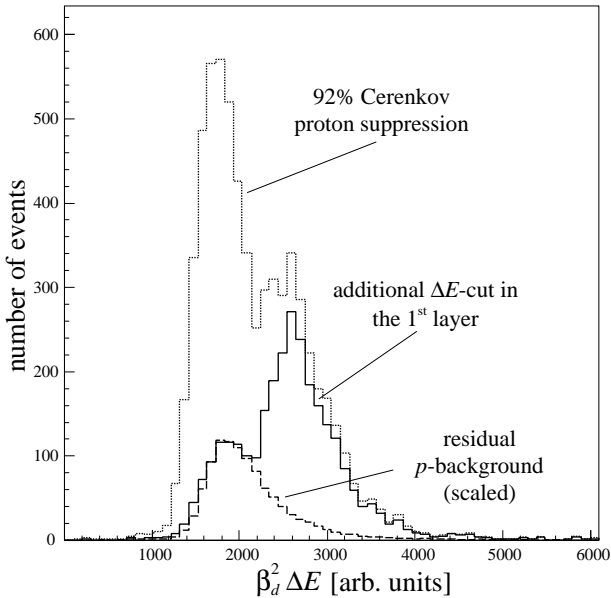


Fig. 3. Energy loss in the second layer of the forward scintillator hodoscope scaled with β_d^2 , where β_d is the deuteron velocity. The dotted histogram shows the result obtained after imposing a 92% proton suppression with the help of the Čerenkov counters. The solid lines result from adding a further ΔE cut using information from the first layer. The residual proton background is shown by the dashed line.

3 Data Analysis

Having identified a spectator proton in the telescope and a deuteron in the forward array and furthermore measured their momenta and directions, one can evaluate the missing mass m_X in the reaction. To clarify the effects of the kinematics, it is sufficient to treat the spectator as being non-relativistic. To order p_{sp}^2 we have then

$$m_X^2 \approx \tilde{m}_X^2 + 2(\mathbf{p}_d - \mathbf{p}) \cdot \mathbf{p}_{\text{sp}} - 2 \left(\frac{E + m_d - E_d}{m_p} \right) p_{\text{sp}}^2, \quad (1)$$

where \tilde{m}_X is the value obtained at $p_{\text{sp}} = 0$. Here p and E are the laboratory momentum and total energy of the incident proton, p_d and E_d those of the produced deuteron, and m_d and m_p the masses of the deuteron and proton respectively. The square of the pn cm energy, s , can be evaluated purely using measurements in the spectator counter and from this Q can be derived:

$$s = (m_d + m_\omega + Q)^2 \approx \tilde{s} + 2pp_{\text{sp}} \cos \theta_{\text{sp}} - \left(\frac{E + m_d}{m_p} \right) p_{\text{sp}}^2, \quad (2)$$

where \tilde{s} is the value for a stationary neutron. Because the telescope is placed around $\theta_{\text{sp}} \approx 90^\circ$, $\partial s / \partial \theta_{\text{sp}}$ is then maximal and so the value of Q depends sensitively upon the determination of the polar angle of the spectator with respect to the beam direction.

Since in our set-up the fast deuteron is measured near the forward direction, the same sort of sensitivity is also found for m_X when using Eq. (1). Now for each beam momentum the beam direction could not be established to much better than 0.1° , and this may induce a systematic shift of a few MeV/c^2 in the value of m_X . On the other hand, in view of the ω width, the uncertainty in the beam momentum ($< 1 \text{ MeV}/c$) is unimportant for both Q and m_X at this level of accuracy. The struck neutron is slightly off its mass shell but the off-shellness is controlled by the spectator momentum and rests small throughout our experiment.

In Fig. 4 we show our results from the first two silicon layers ($70 < p_{\text{sp}} < 91 \text{ MeV}/c$), where the spectator hypothesis should be very good. The angular information is important for the missing mass determination but, in view of the limited statistics, we had to sum over rather wide bins in excess energy. Experience with ω production in proton-proton collisions shows that there is considerable multi-pion production under the ω peak [2]. Without measuring the products of the ω decay, this can only be reliably estimated by comparing data above and below the ω threshold. Two of the four momenta correspond to largely below-threshold measurements and two above, at mean values of Q equal to about 28 and 57 MeV.

There is an indication of a weak ω signal at the highest energy and, in order to evaluate its significance, we have to master the large multipion background over our range of energies. Two different approaches have been undertaken to overcome this problem. In the first, pion production is modelled within a phase-space Monte Carlo description.

The second method is identical to that used in the analysis of the $pp \rightarrow pp\omega$ experiment [2], where the data below ω threshold were taken to be representative of the background above, being merely shifted kinematically due to the changed beam energy such that the upper edges of phase space match. This matching of the ends of phase space can also be used to check the set-up of the system at each momentum. The only significant discrepancy was found at 2.807 GeV/c where, in order to account for a slight displacement observed in the data, 3 MeV/c² has been subtracted from all m_X values at this beam momentum. As will be shown in the next section, the two different analysis methodologies give consistent results within the error bars.

Most of the background can be described by phase space convoluted with the ANKE acceptance, which provides a severe cut at low m_X . It should be noted that the available $np \rightarrow d\pi^+\pi^-$ data in our energy range show the deuteron distribution to be fairly isotropic in the cm system [16]. In the absence of neutron data, we parameterised the total cross section $\sigma(s)$ for the production of N pions in proton-proton collisions by

$$\sigma(s) = A \left(1 - \frac{s_0}{s}\right)^{p_1} \left(\frac{s_0}{s}\right)^{p_2}, \quad (3)$$

where s_0 is the threshold for $N\pi$ production. The exponent p_1 is fixed by phase space, but A and p_2 are free parameters adjusted to reproduce the $pp \rightarrow d(N\pi)$ data for 2, 3 and 4 pion production [17]. The assumption that each of the three contributions follows a $(N + 1)$ -body phase space, undistorted by Δ or ρ resonances, gives a description of the m_X distributions for different beam energies. To model the $pn \rightarrow d(N\pi)$ background, the energy dependence from the pp case has been used to fix the p_i , with the A being adjusted to reproduce simultaneously our experimental distribution at 2.7 GeV/c and the phase-space maximum at 2.9 GeV/c. The relative normalisation between these two momenta was determined from the pd elastic scattering data. The adjusted A values, together with the relative normalisation established from the luminosity measurement, were used to describe the multipion background at 2.6 GeV/c and at 2.8 GeV/c, as shown in Fig. 4.

Our method gives a plausible description of the background under the ω peak at $Q \approx 57$ MeV but any ω signal at $Q \approx 28$ MeV lies close to the maximum of the phase-space acceptance and the evaluation of its strength depends much more critically upon the background assumptions. Nevertheless, within the parametrisation of Eq. (3), it is impossible to describe the phase-space maxima simultaneously at the four energies in Fig. 4 without invoking some ω signal at $Q \approx 28$ MeV.

To describe the ω contribution to the missing mass spectra, we take the $pn \rightarrow d\omega$ matrix element to be constant over the Q -bin so that the cross section follows phase space. This, combined with the decrease of acceptance at large Q , means that the mean value of Q is not quite at the centre of the bin. Other plausible assumptions, such as a constant cross section, would lead to negligible changes in the evaluation of the cross section and mean

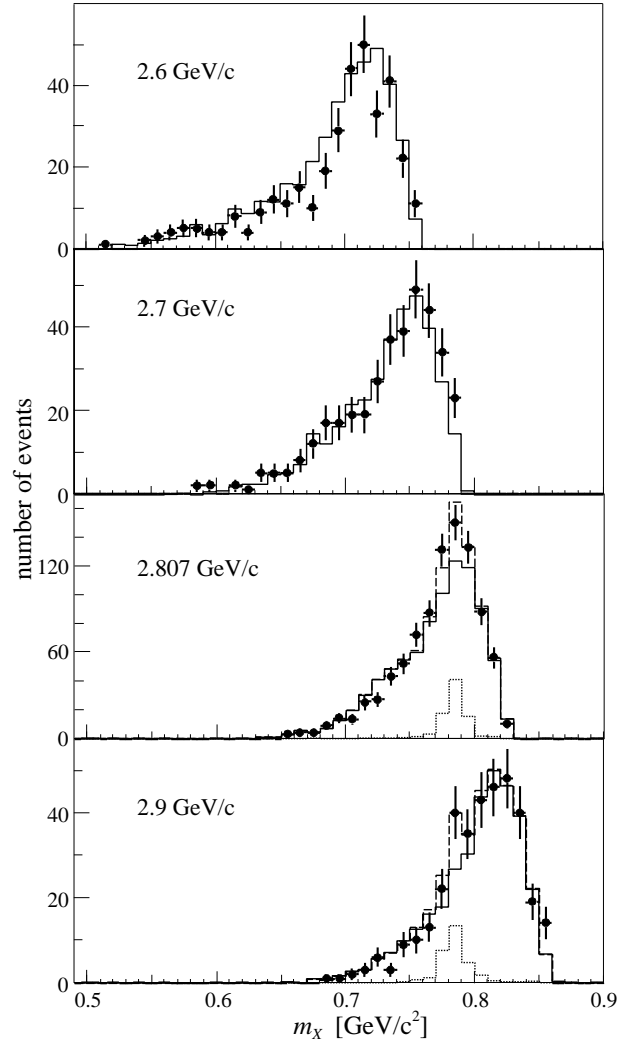


Fig. 4. Missing mass m_X in the $pd \rightarrow p_{\text{sp}}dX$ reaction. Two of the four beam momenta 2.6, 2.7, 2.807, and 2.9 GeV/c are largely below and two above the nominal threshold for ω -production, with excess energies summed over the ranges $-58 < Q < -22$, $-23 < Q < 13$, $8 < Q < 44$, and $42 < Q < 78$ MeV respectively. The solid line is a multipion fit to the data at 2.7 GeV/c and 2.9 GeV/c, as described in the text. There is evidence for an ω signal (simulated as the dashed line) at 2.9 GeV/c, though the result at 2.807 GeV/c depends much more sensitively upon the background simulation.

value of Q . In the simulation of the $pd \rightarrow p_{\text{sp}}d\omega$ reaction, the cross section is smeared over the Fermi motion in the deuteron using the PLUTO event generator [18]. This employs the Hamada-Johnston wave function [19] though, at these small values of spectator momenta, other more realistic wave functions give indistinguishable results. The same event generator is used also for the multipion background.

Turning now to our second approach, the authors of ref. [2] noticed that, apart from the ω signal, the shape of the $pp \rightarrow ppX$ missing mass spectrum varied little with beam energy provided that one looked at the distribution

with respect to the maximum missing mass. More quantitatively, if β and β_n are c.m. velocities at energies T and T_n respectively, the measured momenta and angles of the protons were first transformed, event-by-event, from the laboratory to the c.m. system with the velocity $-\beta$ and then transformed back to the laboratory with the velocity $+\beta_n$. To see to what extent this approach is valid for the ANKE spectrometer, which has a much smaller overall acceptance than that of SPESIII [2], we have reconstructed the missing mass for the copious proton production $pd \rightarrow p_{sp}pX$. The data at the four different beam momenta, kinematically shifted to 2.9 GeV/c and normalised to the same total number of events, are shown in Fig. 5.

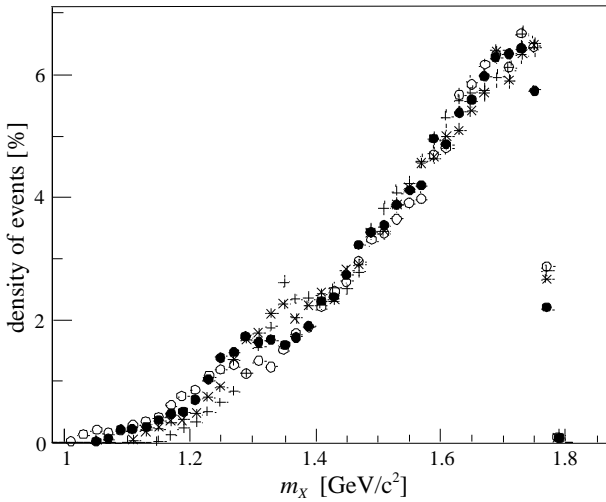


Fig. 5. Missing-mass spectra of the $pd \rightarrow p_{sp}pX$ reaction at 2.6 (crosses), 2.7 (stars), 2.8 (closed circles), and 2.9 GeV/c (open circles) kinematically shifted using the SPESIII procedure [2]. The data are all normalised to the same total of 100%.

It is clear from the figure that for $m_X > 1.4$ GeV/c² the shifted data are in mutual agreement at all beam momenta. For lower missing masses one sees the effect of the production of the $\Delta(1232)$ isobar, whose position in the *shifted* mass scale depends, of course, upon the beam momentum. The figure also nicely illustrates the influence of the ANKE acceptance cut, which strongly favours events close to the maximum missing mass.

When the identical analysis procedure is applied to the $pd \rightarrow p_{sp}dX$ data, the backgrounds away from the ω peak at the different momenta are again found to be completely consistent. An average background could therefore be constructed and this is shown for the two above-threshold momenta in Fig. 6. The differences between the experimental data and constructed background shows evidence for structure in the ω region and these have been fitted to ω peaks whose widths were fixed by the Monte Carlo simulation. The ω masses obtained from the fits at the two momenta, 780 ± 8 and 787 ± 4 MeV/c², do not differ significantly from the expected value.

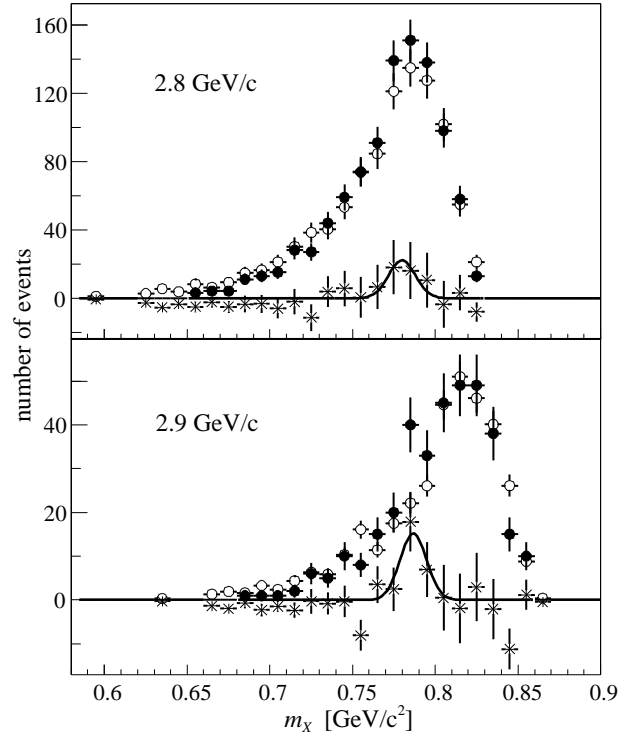


Fig. 6. Missing-mass spectra of the $pd \rightarrow p_{sp}dX$ reaction. The closed circles are the experimental data at 2.8 and 2.9 GeV/c whereas the open circles represent the data at the other momenta shifted using the SPESIII procedure [2]. The differences between the data sets (stars) are fitted to the expected ω -peak shape to yield the measured production cross section.

4 Results

By comparing the residual signal in Fig. 4 with a simulation of ω production over this range of spectator energies and angles, we would conclude from simulated background model that $\sigma_{tot}(pn \rightarrow d\omega) = (2.9 \pm 0.8) \mu\text{b}$ at $Q = (28_{-20}^{+16})$ MeV and $(8.5 \pm 2.8) \mu\text{b}$ at $Q = (57_{-15}^{+21})$ MeV, where the uncertainty in Q reflects the total width of the bin and only the statistical error in the cross section is quoted. The corresponding numbers obtained using the SPESIII background technique, $(2.2 \pm 1.4) \mu\text{b}$ and $(9.4 \pm 3.3) \mu\text{b}$ respectively, are consistent with the first method, though the statistical errors are larger because we had to subtract a background with limited statistics. This contrasts with our first approach where we imposed the condition that the background should be smooth. Averaging the two sets of results, we obtain $\sigma_{tot} = (2.6 \pm 1.6 \pm 2.3) \mu\text{b}$ and $(9.0 \pm 3.2_{-2.5}^{+3.6}) \mu\text{b}$ at the two excess energies. The second, systematic, error bar includes some contribution arising from the ambiguity of the background discussed above but others, such as the uncertainty in the luminosity, are common to both the signal and background.

In view of the limited statistics it might be helpful to quote upper limits resulting from the fits to the count differences shown in Fig. 6. At the 90% confidence level the cross sections at 2.8 and 2.9 GeV/c are below $(7.5 \pm 5) \mu\text{b}$

and $(17 \pm 6) \mu\text{b}$ respectively, where the second figure is the rescaled systematic uncertainty.

One source of systematic uncertainty comes from the restricted angular acceptance of ANKE [11], a problem that becomes more serious with increasing Q . The simulation of the acceptance, illustrated in Fig. 7 for an isotropic production distribution, shows that, while the distribution is fairly flat at 2.8 GeV/c, few events would be accepted close to 90° at 2.9 GeV/c. Although at our energies we might expect S -wave production to dominate, when this acceptance is weighted with the possible pure P -wave angular variations of $\cos^2\theta$ or $\sin^2\theta$, the resulting overall acceptance estimate at 2.9 GeV/c is changed by factors of 1.7 and 0.65 respectively. These are, however, extreme scenarios and a systematic error of half of the difference between these values is a generous estimate of this uncertainty. In more refined experiments, where the statistics will allow us to determine the angular distribution, this limitation will be avoided.

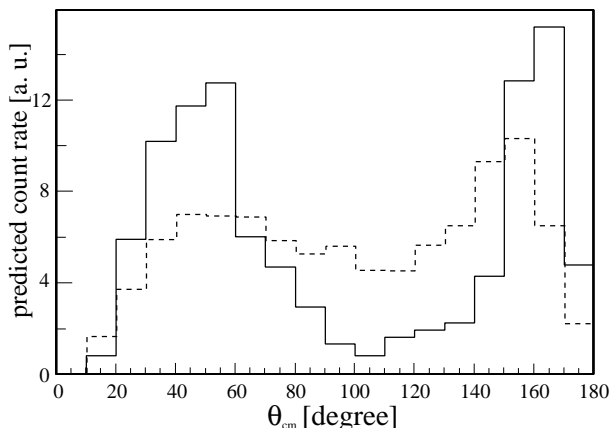


Fig. 7. Predicted angular acceptance for $pd \rightarrow p_{\text{sp}}d\omega$ events at 2.9 GeV/c (solid line) as a function of the deuteron c.m. angle, assuming an isotropic production process. At 2.8 GeV/c (dashed line) the distribution becomes more uniform.

The reduction of flux due to the presence of a second nucleon in the deuteron target (shadowing) has been estimated in the η -production case to be about 5% of the NN cross section [20] and such a correction has been applied to our data. These values are shown in Fig. 8 along with those for the $pp \rightarrow pp\omega$ reaction.

Due to the momentum distribution in the deuteron, the statistics for spectators in the higher range, $8 < T_{\text{sp}} < 22$ MeV, are only about a third of those in the lower range. Nevertheless, the corresponding missing mass spectra are consistent with those shown for the lower spectator energies in Fig. 4, with ω cross sections compatible with our results in Fig. 8.

We have checked our methodology by identifying events corresponding to the $pd \rightarrow p_{\text{sp}}d\pi^0$ reaction at 1.22 GeV/c. Using the same procedures as for the ω analysis, we find $\sigma_{\text{tot}}(pn \rightarrow d\pi^0) = (1.6 \pm 0.3) \text{mb}$ at $Q = (135 \pm 9) \text{MeV}$, where the statistical error is negligible. This value is to be

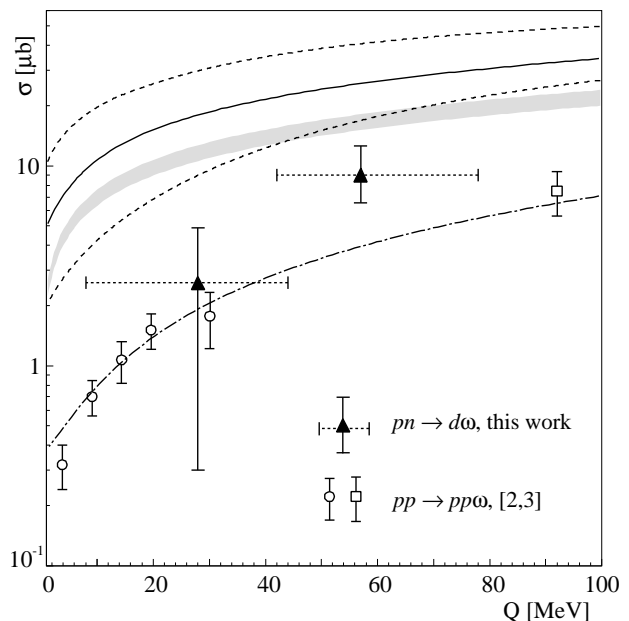


Fig. 8. Total cross sections for ω -production. The $pp \rightarrow pp\omega$ data are taken from SATURNE [2] (open circles) and COSY-TOF [3] (open square), whereas our two $pn \rightarrow d\omega$ points are given by the closed triangles. Only the systematic errors are shown as the statistical errors 1.6 and $3.2 \mu\text{b}$ at the two energies are smaller or comparable in size. The horizontal bars indicate the width of the Q ranges. The dot-dashed curve is the semi-phenomenological fit given in Ref. [2] to the $pp \rightarrow pp\omega$ results taking the ω width into account. If the ratio for $d\omega$ to $pp\omega$ were similar to that for η production [6], one would then obtain the solid curve, which predicts a $pn \rightarrow d\omega$ cross section of over $25 \mu\text{b}$ at 57 MeV. The predictions of the Jülich group depend upon the relative contributions of exchange and production current terms and lie between the two dashed curves [22]. The only other published estimate [23] is shown by the shaded area.

compared to 1.53 mb deduced from a compilation of the isospin-related $pp \rightarrow d\pi^+$ reaction [21].

5 Conclusions

In any meson exchange model, the relative strength of ω production in pp and pn collisions depends sensitively upon the quantum numbers of the exchanged particles. If only a single isovector particle, such as the π or ρ , were exchanged then, neglecting the differences between the initial and final NN interactions, one would expect $\sigma_{\text{tot}}(pn \rightarrow pn\omega)/\sigma_{\text{tot}}(pp \rightarrow pp\omega) = 5$. This would explain most of the 6.5 factor found in the η case [6]. Assuming that the ratio $d\omega$ to $pp\omega$ is as for η production, the parametrisation of the available $pp \rightarrow pp\omega$ data [2, 3] leads to the solid curve, which lies about a factor of three above our data. Another estimate is a little lower but similar in shape [23]. Both curves lie within the extremes of the predictions of the Jülich theory group [22], where the major uncertainty arises from the relative strengths of production and exchange current terms.

Taking our 90% C.L. upper limit on the cross section, augmented by the corresponding systematic uncertainty, would barely bring the data into agreement with the solid line of Fig. 8. Even considering only these upper limits, the model predictions appear higher than the data. Any theoretical overestimation might be explained if there were significant isoscalar exchange, perhaps through the ω itself.

In summary, we have carried out the first measurement of the $pn \rightarrow d\omega$ reaction by detecting the spectator proton from a deuterium target in coincidence with a fast deuteron. Although the data are of very limited statistical significance, they suggest that the cross section lies below the published theoretical predictions.

In order to clarify the situation further, we are constructing second generation silicon telescopes that will increase the acceptance significantly. It would then be of interest to try to extend this study to the ϕ region so that one could investigate the OZI rule in the $I = 0$ channel to see if the deviations are similar to those in the $I = 1$ channel.

The work reported here formed part of the PhD thesis of one of the authors [IL]. We are most grateful to the team of the IKP semiconductor detector laboratory, D. Protić, T. Krings and G. Fiori, who developed and supported the necessary material for our spectator counters. We wish to thank D. Prasuhn, J. Stein, B. Lorentz and the COSY team for carrying out the beam development required by the condition that our detectors are only 5 cm from the circulating proton beam. P. Wieder, W. Borgs and S. Mikirtichiants helped in preparing and performing the experiment. The work has been financially supported by the DFG (436 RUS 113/630/71), the Russian Academy of Science (RFBR02-02-0425) and the FZ-Jülich (COSY-064).

References

1. See for example H. Calén *et al.*, Phys. Lett. **B 366** (1996) 39; J. Smyrski *et al.*, Phys. Lett. **B 474** (2000) 182.
2. F. Hibou *et al.*, Phys. Rev. Lett. **83** (1999) 492.
3. S. Abd El-Samad *et al.*, Phys. Lett. **B 522** (2001) 16.
4. The field is summarised in G. Fäldt, T. Johansson and C. Wilkin, Phys. Scrip. **T99** (2002) 146.
5. H. Calén *et al.*, Phys. Rev. **C 58** (1998) 2667.
6. H. Calén *et al.*, Phys. Rev. Lett. **79** (1997) 2642, *idem* **80** (1998) 2069.
7. K. Hagiwara *et al.*, Phys. Rev. **D 66** (2002) 010001.
8. S. Sawada *et al.*, Nucl. Phys. **A 615** (1997) 277.
9. R. Bilger *et al.*, Nucl. Instr. Meth. **A 457** (2001) 64.
10. H. Dombrowski *et al.*, Nucl. Instr. Meth. **A 386** (1997) 228; A. Khoukaz *et al.*, Eur. Phys. J. **D 5** (1999) 275.
11. S. Barsov *et al.*, Nucl. Instr. Meth. **A 462/3** (2001) 364.
12. I. Lehmann, PhD thesis, University of Cologne, 2003; I. Lehmann *et al.*, Nucl. Instr. Meth. A (*in press*).
13. V. Franco and R. J. Glauber, Phys. Rev. **142** (1966) 1195.
14. N. Dalkhazav *et al.*, Sov. J. Nucl. Phys. **8** (1969) 196.
15. B. Chiladze *et al.*, Part. and Nucl. Lett. **4** (2002) 113.
16. A. Abdivaliev *et al.*, Nucl. Phys. **B 168** (1980) 385.
17. Landolt-Börnstein, **12** (1980) p. 97, reactions 71, 72 and 73.
18. <http://www-hades.gsi.de/computing/pluto/html/PlutoIndex.html>
19. T. Hamada and I.D. Johnston, Nucl. Phys. **34** (1962) 382.
20. E. Chiavassa *et al.*, Phys. Lett. **B 337** (1994) 192.
21. http://gwdac.phys.gwu.edu/analysis/pd_analysis.html
22. K. Nakayama, J. Haidenbauer and J. Speth, Phys. Rev. **C 63** (2001) 015201.
23. V. Grishina *et al.*, Phys. Atom. Nucl. **63** (2000) 1824.